III－137 DRAINED AND UNDRAINED STIFFNESS OF KAOLIN IN TRIAXIAL COMPRESSION

MUKABI, J. Ngaya (Graduate Student, Univ. of Tokyo)
TATSUOKA, Fumio (IIS, Univ. of Tokyo)
HIROSE, Kazuhiko (Formerly, Nihon Univ.)

1. INTRODUCTION: A series of triaxial compression tests were performed to study into the effect of drainage condition on the stress-strain relation of clay, in particular the small strain stiffness in relation to the effect of the stress ratio during consolidation.

2. TESTING PROCEDURE: Specimens were prepared from slurry of kaolin (LL= 82.4%, PI= 43.6). An automated stress path control triaxial system was used which could apply unload/reload cycles with an amplitude of axial deformation of one μm or less at a constant strain rate during monotonic loading[1),2),3)]. All samples were consolidated at an axial strain rate of 0.01%/min either isotropically ($K=\sigma_3'/\sigma_1'=1.0$, I-specimen) or anisotropically (K= 0.64, A-specimen) (Table 1). Except one, the specimens were consolidated to $p'=(\sigma_1'+2\sigma_3')/3=3.0$ kgf/cm^2, while Test ID1 to p'= 2.525 kgf/cm^2. The samples were then sheared under drained or undrained conditions at $\dot{\varepsilon}_1$= 0.01%/min.

3. DISCUSSION OF RESULTS (see Table 1): Fig. 1 shows the stress paths during consolidation and shear. The letters D and U stand for 'drained' and 'undrained'. The same drained stress path at σ_3'= 2.525 kgf/cm^2 was traced in Tests ID1 and AD. The overall stress-strain relations are shown in Fig. 2. The following points may be seen from Figs. 1 and 2: **(1)** The effective stress path in Test AU is located above the failure envelop denoted as CSL, which was reached after large strains in the other tests. It seems that since only about 0.1% of axial strain occurred until CSL was reached in Test AU, the structure formed during anisotropic consolidation was preserved to a large extent when approaching to CSL and this brought the specimen above CSL[3)]. **(2)** When the relationship between the deviator stress q and strain is compared, the initial portion of the relation of Test AD (the part from the point **a** in Fig. 2) is substantially different from that of Test ID1 (i.e., the part from the point **b**). This is also the case in the comparison between Tests IU and AU of the relationship between the stress ratio q/p' and strain. The $q-\varepsilon_1$ relation after a certain stress increment (above the point **c**) in Test AD becomes similar to that above the point **d** in Test ID1 and the maximum strength q_{max} is virtually the same between Tests ID1 and AD.

When the initial portions of the relationships between Δq (the change in q) and strain are compared, the difference between A- and I-specimens is much less. Figs. 3 and 4 compare the relationships between Δq and ε_1 or the shear strain ($\gamma=\varepsilon_1-\varepsilon_3$) of the drained and undrained specimens consolidated to p'= 3.0 kgf/cm^2. It may be seen that between A- and I-specimens, these $\Delta q-\varepsilon_1$ relations are much more similar than the $q-\varepsilon_1$ relations shown in Fig. 2. The difference in Δq and ε_1 (γ) relations among the four specimens becomes smaller as the strain level becomes lower. This point is better seen in the relations at ε_1 less than 0.003 or 0.005% shown in Fig. 5.

Fig. 5 shows that the behaviour at strains less than about 0.001% is linear and also elastic. The maximum Young's modulus E_{max} was determined in the region of very small strains. Note that E_{max} for Test ID1 is slightly lower than that of Test ID2 due to a lower p' at consolidation (see Table 1). The values of E_{max} was almost independent of the stress ratio during consolidation. The values of E_{max} for the undrained tests were slightly larger than those of for the drained tests. This can be explained as follows. The shear modulus is more stress-path independent than the Young's modulus. Therefore, even for the same G_{max}, the value of $E_{max}=2(1+\nu)\cdot G_{max}$ is a function of the Poisson's ratio ν, which is 0.5 for undrained tests and is much smaller for drained tests. The values of ν at very small strains for I- and A-specimens were estimated as 0.1 and 0.2, respectively. Then, the values of G_{max} obtained as $E_{max}/2(1+\nu)$ became slightly larger for the drained tests (Table 1), probably due to that with shearing, p' decreased in the undrained tests while it increased in the drained tests.

4. CONCLUSIONS: The initial shear modulus defined from the start of shearing of clay is rather independent of the stress ratio during consolidation and the drainage conditions, while the stiffness at larger strain levels (particularly at γ>1%) is influenced largely by the two factors and the tangent stiffness tends to depend on the current effective stresses and the drained conditions.

REFERENCES: 1) Mukabi,J.N., Ampadu,S.K., Tatsuoka,F., Sato,T. and Hirose,K. (1991a): Small strain stiffness and elasticity of clays in monotonic loading triaxial compression, Proc. Symp. on triaxial testing methods, Japanese Society of SMFE, Tokyo, pp.257-264. 2) Sato,T.,Ampadu,S.I.K., Mukabi,J.N. and Tatsuoka,F. (1991): Development of systems for strain-controlled cyclic loading with very small amplitudes, Proc. Annual Syposium of Japanese Society of SMFE, Nagano. 3) Mukabi,J.N., Tatsuoka,F., and Hirose,K. (1991b): Effext of strain rate on small strain stiffness of kaolin in CU triaxial compression, Proc. Annual Syposium of Japanese Society of SMFE, Nagano.

TABLE 1 Summary of the test results

STAGE	NAME OF TEST	ID2	AD	IU	AU	ID1
CONSOLI-DATION	$K_c=(\sigma_r'/\sigma_a')$	1.00	0.64	1.00	0.64	1.00
	(1) w_{CP}(%)	66.38	66.40	62.07	64.40	64.93
	(2) w_{FC}(%)	50.75	50.92	48.49	48.28	52.38
	(3) w_{FS}(%)	44.32	46.96	48.49	48.28	45.14
	p_0'(kgf/cm²)	3.000	3.000	3.000	3.000	2.525
	σ_{rc}'(kgf/cm²)	3.000	2.526	3.000	2.526	2.525
	q_0(kgf/cm²)	0	1.421	0	1.421	0
SHEAR-ING	ε_v(%)	7.732	4.710	0	0	8.560
	q_{max}(kgf/cm²)	2.32	1.90	1.10	1.79	1.900
	E_{max}(kgf/cm²)	913	973	1095	1090	798
	G_{max}(kgf/cm²)	415	405	365	363	332
	(4) ϕ'(°)	16.0	15.8	15.2	18.44	15.2

(1) w_i: Pre-consolidation WC
(2) w_{cf}: Post-consolidation WC
(3) w_{sf}: Post-shear WC
(4) ϕ': Angle of friction,

$\sin^{-1}\{(\sigma_1 - \sigma_3)/(\sigma_1 + \sigma_3)\}_{max}$

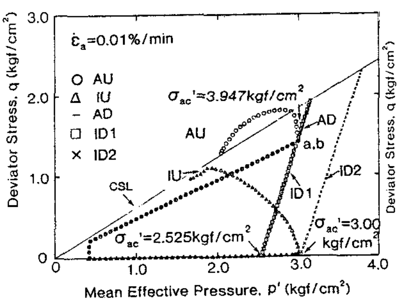

Fig. 1 Stress paths

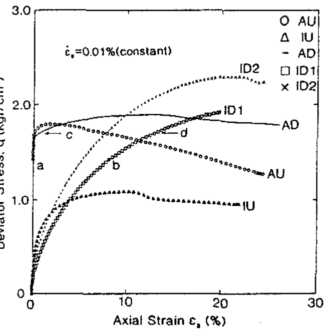

Fig. 2 q−ε₁ relations

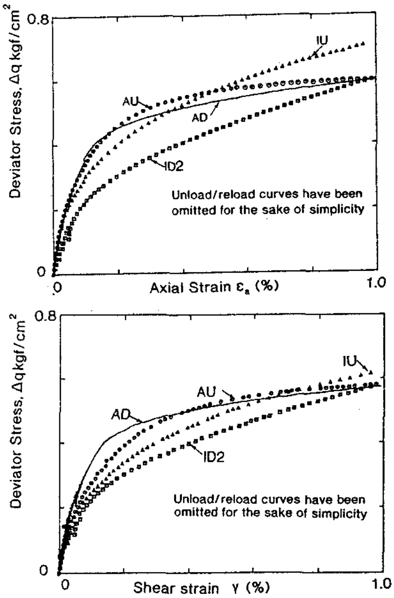

Fig. 3 q−ε₁(γ) relations

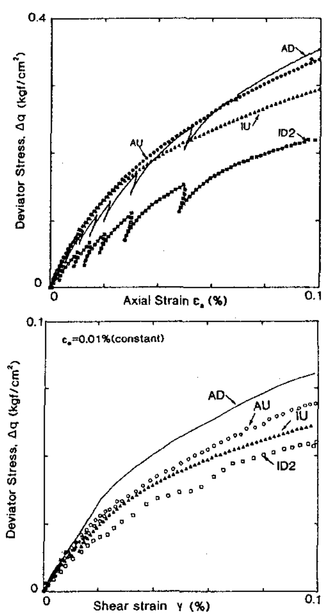

Fig. 4 q−ε₁(γ) relations

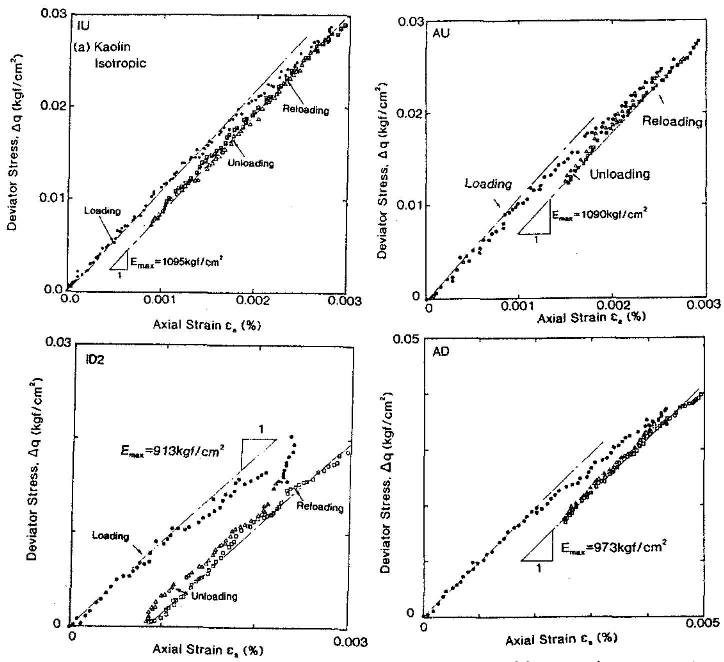

Fig. 5 q−ε₁ relations at very small strains